PHYSICAL REVIEW B VOLUME 39, NUMBER 4 1 FEBRUARY 1989

Fermi-surface geometry and pressure effects on the spin-fluctuation contributions to the specific heat: Anisotropic spin-fluctuation model for heavy-fermion UPt_3

D. Ihle and H. Fehske
Karl-Marx-Universität, Sektion Physik, Karl-Marx-Platz, DDR-7010 Leipzig, German Democratic Republic
(Received 11 January 1988; revised manuscript received 27 July 1988)

On the basis of an uniaxially anisotropic and nonparabolic band model, the effects of Fermi-surface (FS) anisotropy and topology and of hydrostatic pressure on the spin-fluctuation (SF) contributions to the low-temperature specific heat of exchange-enhanced paramagnetic metals are investigated in the framework of paramagnon theory. The model describes different types of SF; for the closed FS a parameter region is found in which there is a coexistence of anisotropic ferromagnetic and antiferrromagnetic SF. In this region and for the open FS a linear relation between the SF-mediated mass enhancement and the Stoner enhancement factor can be obtained which results in the pressure-dependent scaling of the SF parameters and the magnetic susceptibility in terms of only one parameter. For either FS topology the $T^3 \ln T$ law holds, where the amplitude is enlarged compared with the parabolic band model and the range of validity increases with FS anisotropy. Comparing theory with experiments, an anisotropic SF model for UPt_3 is proposed which describes the coexistence of antiferromagnetic SF along the hexagonal axis and ferromagnetic SF in the basal planes and may explain the specific heat, magnetic susceptibility, and neutron scattering experiments.

I. INTRODUCTION

In the theory of heavy-fermion metals,[1,2] the microscopic descriptions of the quasiparticle formation in narrow renormalized bands at very low temperatures and of the effective quasiparticle interactions mediated by the exchange of low-frequency quantum fluctuations, such as the superconducting pairing interaction in $UPt_3(T_c \simeq 0.5$ K) and $UBe_{13}(T_c \simeq 0.9$ K), are fundamental problems, about which there is considerable controversy. For the solution of those problems it is necessary to study in more detail the nature of the possible quantum fluctuations in the normal phase. This may allow the possibility of deciding which fluctuations are relevant for the explanation of the various experiments, whereby the study of pressure effects is an important means.

Let us consider, for example, the low-temperature specific heat C_v of heavy-fermion UPt_3. This reveals, besides a large γT term, a $T^3 \ln T$ contribution which was interpreted in terms of ferromagnetic (FM) spin fluctuations (SF's) in the framework of paramagnon theory[1,3,4] and Fermi-liquid theory.[5–7] Recently, the $T^3 \ln T$ law was derived from Kondo[8] and Anderson lattice[8–10] models. Auerbach and Levin[8] have analyzed, within their Kondo boson theory (describing long-wavelength hybridization and f-level fluctuations), the pressure-dependent C_v and magnetic susceptibility data, and have questioned the FM SF picture for UPt_3. On the other hand, neutron scattering experiments[11,12] yield evidence for antiferromagnetic (AFM) SF's along the hexagonal axis (which may be described by the Kondo boson model[13]) and for FM SF's within the basal planes.[12] Very recently, long-range AFM order in UPt_3 below 5 K was found.[14]

One common feature of all the long-wavelength fluctuation theories concerned with contributions to C_v beyond the γT term (which for the most part are SF theories for nearly or weakly FM metals[15]) is the assumption of a spherical Fermi surface (FS) or of isotropic small-wave-vector expansions of the response function. By this assumption the $T^3 \ln T$ term can be easily evaluated. On the other hand, the theories concerned with AFM SF's (also based on isotropic small-wave-number expansions around the wave vector at which the static susceptibility has a maximum) do not give rise to a $T^3 \ln T$ law at very low temperatures.[16] However, the current applications of fluctuation theories, based on isotropic models, to heavy-fermion metals[3–10] are too simple to take into account the crystal and band structures. For example, UPt_3 (hexagonal $MgCd_3$-type structure) reveals a strong uniaxial anisotropy in many macroscopic properties (e.g., thermal expansion, magnetic susceptibility, electrical resistivity[7]) and an anisotropic FS.[17]

The FS anisotropy and topology may result in qualitative effects on the fluctuation contributions to various macroscopic properties. In our preceding papers,[18] hereafter referred to as I and II, this was demonstrated for the SF-mediated mass enhancement in the framework of paramagnon theory, where we have considered a uniaxially anisotropic and nonparabolic single-band model and calculated the response function $\chi_0(\mathbf{q},\omega)$ of noninteracting electrons at zero temperature. In this work we extend our previous investigations of FS geometry effects on SF phenomena as follows. Using paramagnon theory (based on the Hubbard model) and the anisotropic band dispersion of I we calculate, for the first time, the FS anisotropy and topology effects on the SF contributions to C_v beyond the γT term, in particular on the $T^3 \ln T$ law. Based on new results for the full $\mathbf{q}$ dependence of $\chi_0(\mathbf{q})$

for the closed FS, we give a physical picture of coexistence of AFM and FM SF's and evaluate the SF-mediated mass enhancement as a function of the Stoner factor. Moreover, we study the pressure dependence of the SF model parameters and compare our results with several experiments on UPt_3. The main goals of this paper are (i) to determine the characteristics of the $T^3 \ln T$ law in dependence on the FS geometry and (ii) to suggest an anisotropic SF model for UPt_3.

In Sec. II we present the model describing the different kinds of exchange-enhanced SF's. In Sec. III we calculate the SF contributions to C_v for both the closed and the open FS. The pressure effects on the model parameters and pressure-dependent scaling relations are derived in Sec. IV. The most important point of our discussion (Sec. V) is concerned with the applicability of our extended SF theory to UPt_3. We suggest an anisotropic SF model for UPt_3 (Sec. V C) which describes the coexistence of AFM and FM SF's and may explain the specific heat, magnetic susceptibility, and neutron scattering experiments.

II. MODEL

For the description of FS geometry effects on low-frequency SF's we start from the uniaxially anisotropic single-band model for noninteracting quasiparticles[18]

$$\varepsilon_{\mathbf{k}} = \tfrac{1}{2}(k_x^2 + k_y^2) - \alpha \cos k_z \ , \qquad (1)$$

where $\alpha = 2t_{\parallel} m_b d^2 \hbar^{-2} > 0$ ($t_{\parallel}$ is the tight-binding transfer integral between nearest neighbors on the z axis separated by d, and m_b is the band mass in the effective-mass approximation for the dispersion in the k_x-k_y plane), k_z lies in the first Brillouin zone, $-\pi \le k_z \le \pi$. In (1) the wave-vector components and the energy are measured in units of d^{-1} and $\hbar^2(m_b d^2)^{-1}$, respectively.

From (1) one gets the FS, which we characterize by the FS anisotropy and topology parameter $\xi = 1 + \varepsilon_F/\alpha$ (ε_F is the Fermi energy). In Fig. 1 the FS for different ξ values

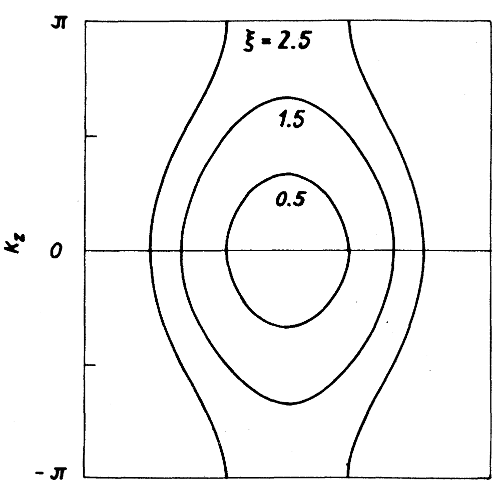

FIG. 1. Fermi surfaces (projected on the k_z-k_x plane) of the model (1).

is sketched in the k_x-k_y plane. The intersection of the FS with the $k_z = 0$ plane is a circle of diameter $d_{\perp} = \sqrt{8\alpha\xi}$, and the maximal extension of the FS in the z direction is $d_{\parallel} = 2\cos^{-1}(1-\xi)\Theta(2-\xi) + 2\pi\Theta(\xi-2)$. In our anisotropic FS model a topological transition from the closed $(0<\xi<2)$ to the open $(\xi>2)$ FS can be described. Let us emphasize that the prolate-ellipsoid-like closed FS with $\xi<1$ and $\xi>1$ (Fig. 1) give rise to qualitatively different properties of $\chi_0(\mathbf{q})$ (Appendix A).

The single-spin density of states $N_0(\varepsilon_F)$ of the noninteracting quasiparticles at ε_F is given by $N_0(\varepsilon_F) = \Omega d_{\parallel}/4\pi^2 d^3$ (Ω volume of the crystal). For later purposes it is convenient to rewrite $N_0(\varepsilon_F)$ in terms of the number of quasiparticles $N_e = \Omega\Omega_F/4\pi^3$ (Ω_F is the volume enclosed by the FS). We get (in nonreduced units, $\xi = 1 + \varepsilon_F/2t_{\parallel}$)

$$N_0(\varepsilon_F) = \frac{\Omega m_b}{4\pi^2\hbar^2 d} d_{\parallel} = [2\varepsilon_F g(\xi)]^{-1} N_e \ , \qquad (2)$$

where

$$g(\xi) = 1 + [\xi(2-\xi)]^{1/2}[(\xi-1)\cos^{-1}(1-\xi)]^{-1}\Theta(2-\xi) \ .$$

Now we consider an exchange-enhanced paramagnetic metal at very low temperatures which shows no magnetic instability down to zero temperature. We describe this by the Hubbard model (with intrasite quasiparticle interaction U) with the band dispersion (1). In the application to heavy-fermion "spin fluctuators" (e.g., UPt_3, UAl_2, USn_3) we consider the Hubbard model, in the spirit of renormalized band theory (hybridization model), as an effective model for the narrow heavy-quasiparticle band at the Fermi energy including a small quasiparticle interaction U, as discussed by Fulde *et al.*[2] However, we assume that the quasiparticle mass described by the band term does not contain the SF contribution.

Assuming small values of U we treat the SF's in the random-phase approximation (RPA). As a characteristic measure for the strength of SF effects, we introduce the Stoner enhancement function

$$S(\mathbf{q}) = \chi(\mathbf{q})\chi_0^{-1}(\mathbf{q}) = [1 - I\chi_0(\mathbf{q})]^{-1} \ , \qquad (3)$$

where $I = U/N$. The enhancement of macroscopic quantities is mainly determined by SF's with wave vectors for which $S(\mathbf{q})$ is large. We consider the metal to be not necessarily in the extreme nearly magnetic limit, i.e., we also take into account moderate values of $S(\mathbf{q})$.

From (1) we calculate (Appendix A) the anisotropic static susceptibility $\bar{\chi}_0(\mathbf{q}) = \chi_0(\mathbf{q})/\chi_0(0)$, where $\bar{\chi}_0(\mathbf{q}) = \bar{\chi}_0(q_{\perp}, q_{\parallel})$, $q_{\perp}^2 = (q_x^2 + q_y^2)/\alpha$, $q_{\parallel} = |q_z|$, and $\chi_0(0) = N_0(\varepsilon_F)$. The properties of $\bar{\chi}_0(\mathbf{q})$ allow the description of different kinds of exchange-enhanced SF's. For $0<\xi<1$ the maximum of $\bar{\chi}_0(\mathbf{q})$ at $\mathbf{q}=0$ gives rise to FM SF's with wave vectors around $\mathbf{q}=\mathbf{0}$ and with the Stoner factor $S \equiv S(0) = [1 - IN_0(\varepsilon_F)]^{-1}$ (paramagnons). For $\xi>2$ the plateau of $\bar{\chi}_0(\mathbf{q})$ in the volume Ω_c results in exchange-enhanced SF's with wave numbers up to the boundary of Ω_c.

Let us consider in more detail the nature of SF's in the closed-FS region $1<\xi<2$, where $\bar{\chi}_0(\mathbf{q})$ exhibits a maximum at $\mathbf{Q}=(0,0,\pi)$. Figure 2(a) shows $\bar{\chi}_0(\mathbf{q})$ for $\xi=1.1$, and in Fig. 2(b) the corresponding Stoner function $S(\mathbf{q})=S[S-(S-1)\bar{\chi}_0(\mathbf{q})]^{-1}$ with $S=4$ is depicted. For the characterization of SF's we consider the behavior of $S(\mathbf{q})$ along a given $\mathbf{q}$ direction. The SF's in this direction, which yield a considerable exchange enhancement, have wave numbers for which $S(\mathbf{q})$ deviates only slightly from its maximum value. Among the exchange-enhanced SF's characterized in this way, there occur two special types of SF's: (i) Because $S(\mathbf{q})$ has a maximum at the AFM ordering vector $\mathbf{Q}$, there exist exchange-enhanced SF's with wave vectors in the neighborhood of $\mathbf{Q}$ and with the enhancement factor $S(\mathbf{Q})$; i.e., we have AFM SF's along the anisotropy axis. (ii) Considering $\mathbf{q}$ directions, where $S(\mathbf{q})$ has a maximum at $\mathbf{q}=0$, the smallest wave-number region in which $S(\mathbf{q})$ only slightly deviates from S is found for $\mathbf{q}$ in the q_x-q_y plane; that is, for those $\mathbf{q}$ directions the maximum of $S(\mathbf{q})$ is most pronounced. Accordingly, we get FM SF's perpendicular to the anisotropy axis with wave numbers around $|\mathbf{q}|=0$ and with $S<S(\mathbf{Q})$. The upper bound S_m for the possible values of S results from the condition that there is no AFM instability $[S^{-1}(\mathbf{Q})>0]$; we get

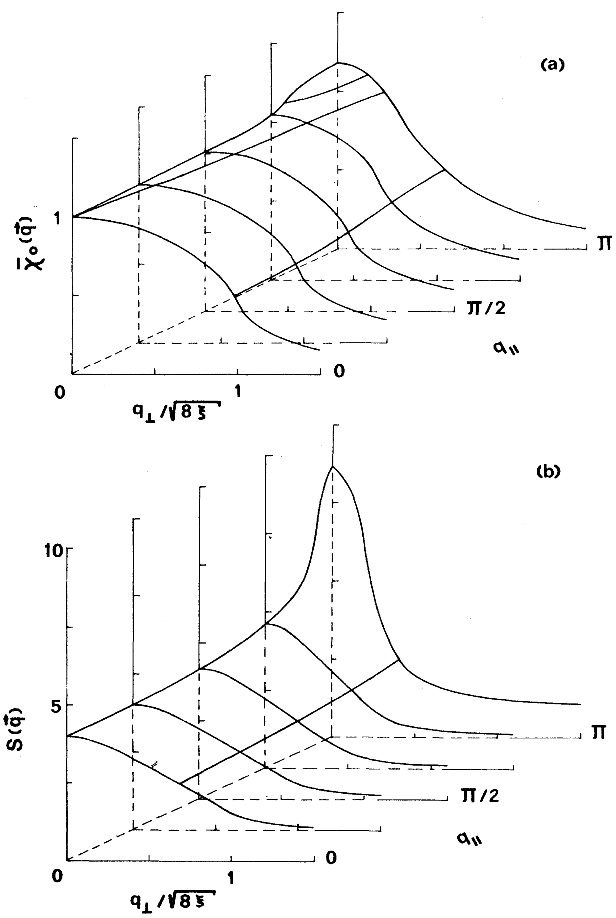

FIG. 2. (a) Static susceptibility for the closed FS with $\xi=1.1$; (b) corresponding Stoner function $S(\mathbf{q})$ for $S=4$.

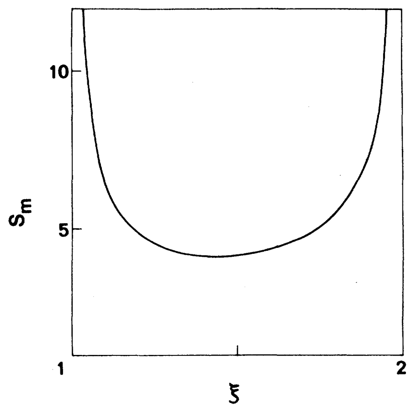

FIG. 3. Upper bound for the Stoner factors in the coexistence region of ferromagnetic and antiferromagnetic SF's.

$$S<S_m=\bar{\chi}_0(0,\pi)[\bar{\chi}_0(0,\pi)-1]^{-1} . \tag{4}$$

By (A3), S_m as a function of ξ is shown in Fig. 3. We see that S can take large enough values. Thus, we obtain a coexistence of anisotropic AFM and FM SF's with different enhancement factors, where S is bounded by S_m.

III. SPIN-FLUCTUATION CONTRIBUTIONS TO THE SPECIFIC HEAT

A. Basic equations

In the RPA for the Hubbard model, the exchange-enhanced contributions of transverse and longitudinal SF's to the thermodynamical potential in the paramagnetic phase are given by[19]

$$\Delta\Omega=\tfrac{3}{2}T\sum_{\mathbf{q},\omega_n}\{\ln[1-I\chi_0(\mathbf{q},i\omega_n)]+I\chi_0(\mathbf{q},i\omega_n)\} , \tag{5}$$

where $\omega_n=2n\pi T$ ($k_B=\hbar=1$). In the low-temperature limit we neglect, as usually done, the rather weak temperature dependence of the spin susceptibility χ_0 given, accordingly, by (A1). Transforming the ω_n sum into an integral over real frequencies and using the standard approximations $\mathrm{Re}\chi_0(\mathbf{q},\omega)\simeq\chi_0(\mathbf{q})$, $\mathrm{Im}\chi_0(\mathbf{q},\omega)\simeq\omega u(\mathbf{q})$ for $\omega/|\mathbf{q}|\ll 1$, we derive the SF contributions to the low-temperature specific heat,

$$\Delta C_v=\frac{3}{\pi}\int_0^\infty dx\, x[2n'(x)+xn''(x)] \times\sum_{\mathbf{q}}\{\tan^{-1}[ITxS(\mathbf{q})u(\mathbf{q})]-ITxu(\mathbf{q})\} , \tag{6}$$

where $n(x)=(e^x-1)^{-1}$. It is convenient to separate (6) into a term linear in temperature and a nonlinear contribution. We obtain

$$\frac{\Delta C_v}{C_{v0}}=\lambda_{\rm SF}+\frac{9}{2\pi^3}\frac{I^3}{N_0(\varepsilon_F)}T^2\int_0^\infty dx\, x^4 n'(x)\sum_{\mathbf{q}}[S(\mathbf{q})u(\mathbf{q})]^3\{1+[ITxS(\mathbf{q})u(\mathbf{q})]^2\}^{-1}\ ,$$
$$\lambda_{\rm SF}=\frac{3I}{2\pi N_0(\varepsilon_F)}\sum_{\mathbf{q}}u(\mathbf{q})[S(\mathbf{q})-1]\ , \tag{7}$$

where $C_{v0}=\gamma_0 T$ and $\gamma_0=\frac{2}{3}\pi^2 N_0(\varepsilon_F)$. In order to accentuate the FS geometry effects on ΔC_v and for the purpose of a comparison, in Appendix B we evaluate ΔC_v in the parabolic-band case. For the calculation of the SF contributions (7) we restrict the $\mathbf{q}$ integration by a cutoff energy (ε_c) surface with the symmetry of the FS. We get

$$\frac{\Delta C_v}{C_{v0}}=\lambda_{\rm SF}+\frac{36}{\pi}\left[\frac{2\pi}{d_\parallel}\right]^4\xi^2(S-1)\tau^2 J(\tau)\ , \tag{8}$$

$$\lambda_{\rm SF}=\frac{3}{\pi}\left[\frac{2\pi}{d_\parallel}\right]^2\frac{(S-1)}{S}\int_0^{q_{\parallel c}}dq_\parallel\int_0^{q_{\perp c}}dq_\perp q_\perp \bar{u}(\mathbf{q})[S(\mathbf{q})-1]\ , \tag{9}$$

$$J(\tau)=\int_0^\infty dx\, x^4 n'(x)\int_0^{q_{\parallel c}}dq_\parallel\int_0^{q_{\perp c}}dq_\perp q_\perp\left[\bar{u}(\mathbf{q})\frac{S(\mathbf{q})}{S}\right]^3\left[1+\left[\frac{4\pi^2}{d_\parallel}\xi x\tau\bar{u}(\mathbf{q})\frac{S(\mathbf{q})}{S}\right]^2\right]^{-1}\ , \tag{10}$$

where

$$\tau=T/\bar{T}_F,\quad \bar{T}_F=\frac{\varepsilon_F\xi}{(S-1)(\xi-1)}\ ,$$
$$q_{\parallel c}=\cos^{-1}(-\varepsilon_c)\Theta(1-\varepsilon_c)+\pi\Theta(\varepsilon_c-1)\ ,$$
$$q_{\perp c}=[2(\varepsilon_c+\cos q_\parallel)]^{1/2},\quad \varepsilon_c=q_c^2\xi-1\ ,$$

and $\bar{u}(\mathbf{q})$ is given in Appendix A. We have expressed ε_c by the parameter q_c, in analogy to the parabolic-band case ($\varepsilon_c=q_c^2\varepsilon_F$, cf. Appendix B). As can be seen from (8)–(10) and (2), besides the parameters ε_F, γ_0 (or N_e/mol), S, q_c, also appearing in the parabolic band model, our SF model contains the additional FS geometry parameter ξ. For the numerical evaluation of (9) and (10) we approximate the function $\bar{u}(\mathbf{q})$ by its expansion for $|\mathbf{q}|\ll 1$ (Appendix A).

B. Mass enhancement

We consider the SF contributions to the linear C_v coefficient given, from (7), by $\gamma=\gamma_0(1+\lambda_{\rm SF})$. We take $1+\lambda_{\rm SF}$ to define the SF mass enhancement. In the application to heavy-fermion "spin fluctuators" (cf. Sec. II), $\lambda_{\rm SF}$ describes the SF-mediated mass correction to the heavy-quasiparticle band mass. In II we have found that $\lambda_{\rm SF}$ crucially depends on the FS topology: Whereas the dominant contribution to $\lambda_{\rm SF}$ for large S in the region $0<\xi<1$ behaves like $\lambda_{\rm SF}\propto\ln S$, for $\xi>2$ the proportionality $\lambda_{\rm SF}\propto S$ holds.

Here, we focus our attention on the behavior of $\lambda_{\rm SF}(S)$ in the closed-FS region $1<\xi<2$, where exchange-enhanced AFM and FM SF's coexist (Sec. II). In order to treat all SF contributions to $\lambda_{\rm SF}$ simultaneously, in the numerical evaluation of (9) we use the full $\mathbf{q}$ dependence of $S(\mathbf{q})$. For the AFM SF's with wave vectors around $\mathbf{Q}$, $\bar{u}(\mathbf{q})$ takes finite values so that $\lambda_{\rm SF}$ remains finite as $S(\mathbf{Q})\to\infty$,[16] i.e., as $S\to S_m$. Taking, tentatively, $q_c=1.6$,[19] the function $\lambda_{\rm SF}(S)$ for $S\le S_m$ (Fig. 3) and for two ξ values is plotted in Fig. 4. With increasing ξ, the dependence of $\lambda_{\rm SF}$ on S varies from a nearly linear increase for all $S<S_m$ to a stronger than linear increase as S approaches S_m, where near the topological transition the mass enhancement at S_m becomes very large.

C. $T^3\ln T$ law

Now we evaluate numerically the SF contributions (8) to C_v beyond the γT term, where we take $S(\mathbf{q})=S$ as a reasonable approximation[19] (cf. Sec. V B). Our results for $-J$ with $q_c=1.6$ and different ξ values are plotted, as functions of $\ln(\bar{T}_F/T)$, in Fig. 5. For $T<T_m\simeq\frac{1}{12}\bar{T}_F$ we obtain the straight line $J=c(\xi)+a(\xi)\ln\tau$. That means, irrespective of the FS anisotropy and topology, the dominant SF contribution to C_v beyond γT obeys the $T^3\ln T$ law. From $\bar{T}_F=\alpha\xi/(S-1)$ we see that, for fixed α, the range of validity of the $T^3\ln T$ law (T_m) increases linearly with ξ, i.e., with the FS anisotropy. From (8), (2), and the results for $c(\xi)$ and $a(\xi)$ we obtain

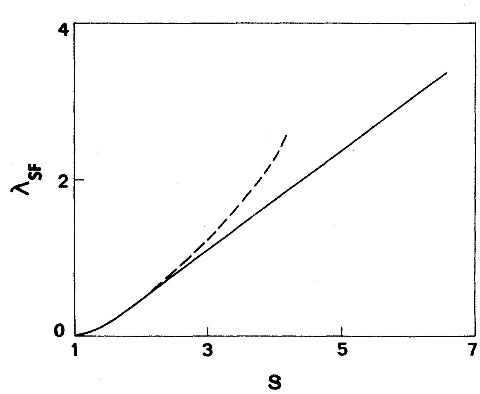

FIG. 4. SF-mediated mass enhancement. Solid curve, $\xi=1.1$; dashed curve, $\xi=1.5$.

$$C_v = \gamma T + \delta T^3 \ln \left[\frac{T}{T_{SF}} \right] \quad \text{for } T < T_m \simeq \tfrac{1}{12} \overline{T}_F \; ,$$

with

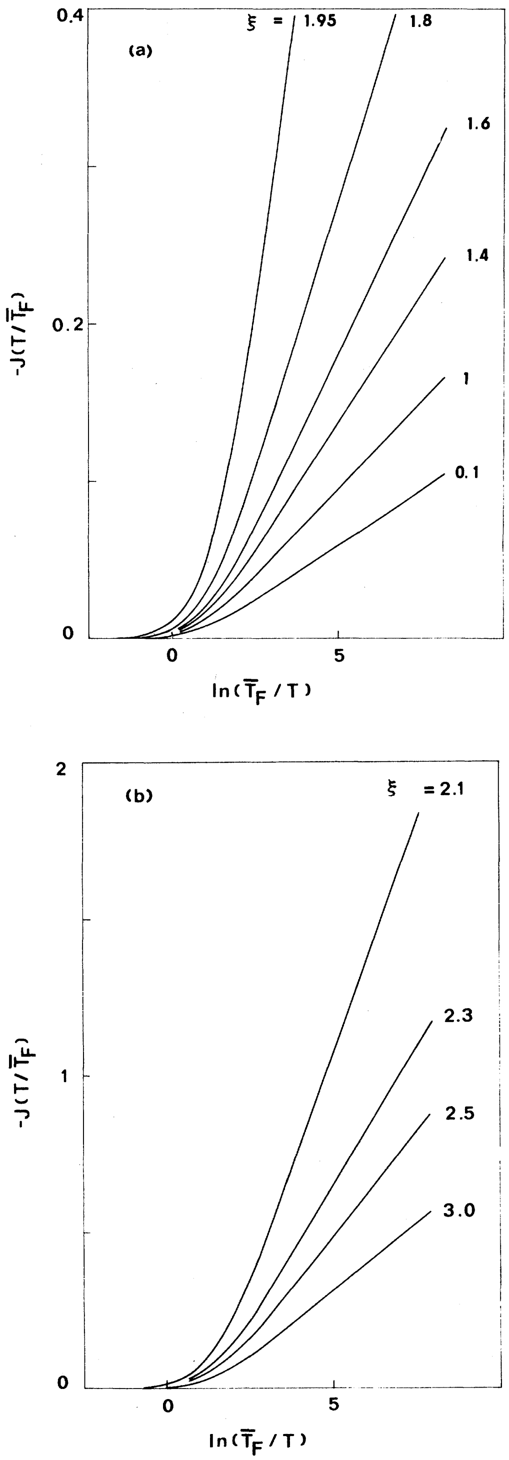

FIG. 5. Integral $-J(T/\overline{T}_F)$ [Eq. (10)] for (a) $\xi<2$ and (b) $\xi>2$.

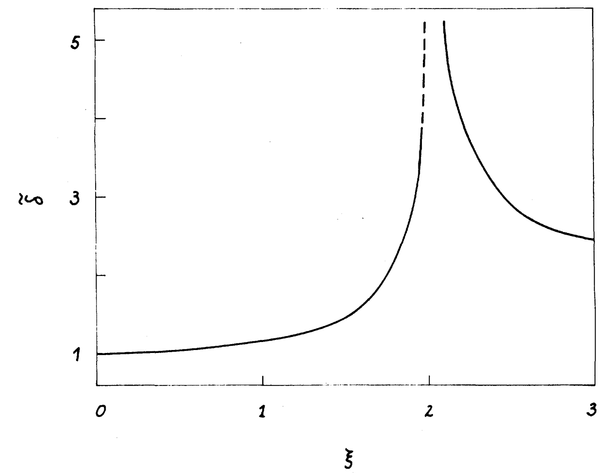

FIG. 6. Function $\tilde{\delta}(\xi)$ according to Eq. (12).

$$\delta = \frac{y}{T_{SF}^3}, \quad T_{SF} = b(\xi)\overline{T}_F \; ,$$

$$y = 12\pi b^3(\xi) A(\xi) B(\xi) N_e k_B \text{ mol}^{-1} \; , \tag{11}$$

$$A(\xi) = \left[\frac{2\pi}{d_{\parallel}} \right]^4 \xi^2 a(\xi), \quad B(\xi) = \xi[(\xi-1)g(\xi)]^{-1} \; ,$$

where $B(0)=\frac{3}{2}$ and $B(1)=\pi/2$. The function $b(\xi) = \exp[-c(\xi)/a(\xi)]$ slightly decreases from $b(\xi<1) \simeq \frac{1}{2}$ to $b(\xi>2) \simeq \frac{1}{4}$, and y is nearly constant (2.3 to $2N_e k_B$ mol^{-1}) up to $\xi \simeq 1.5$.

Let us consider the FS geometry effect on the magnitude of the $T^3 \ln T$ coefficient δ. For this purpose we compare δ with the parabolic-band result $\delta^{(p)}$ following from (B1) (and expressed in terms of N_e, $N_0^{(p)}(\varepsilon_F) = 3N_e/4\varepsilon_F^{(p)}$). With the identification $\varepsilon_F + 2t_{\parallel} = \varepsilon_F^{(p)}$ we get

$$\tilde{\delta} \equiv \frac{\delta}{\delta^{(p)}} = \frac{640}{\pi^5} A(\xi) B(\xi) \; . \tag{12}$$

The function $\tilde{\delta}(\xi)$ is shown in Fig. 6. The FS anisotropy induces an increase of δ compared with the parabolic result, where $\tilde{\delta}$ increases appreciably with ξ in the closed-FS region $1<\xi<2$. The anomaly of $\tilde{\delta}$ in the vicinity of the topological transition ($\xi=2$), is due to the neglect of the temperature dependence of the spin susceptibility in (5). As discussed by Lifshitz,[20] the anomalies of thermodynamical quantities, occurring near the topological transition at $T=0$, are smeared out for finite temperatures.

IV. PRESSURE EFFECTS

The study of hydrostatic-pressure (p) effects on the fluctuation contributions to macroscopic quantities may give important information on the microscopic fluctuation mechanisms. For UPt_3 the p-dependent data were considered by Auerbach and Levin[8] as evidence against the applicability of the paramagnon model, whereas Brodale *et al.*[4] have based their fit on that model. In this section we investigate the p dependence of the SF model parameters in (11).

Let us first consider the p dependence of ξ. Deriving the effective-mass approximation for the dispersion (1) in the xy plane from the tight-binding approximation, we have $m_b \propto (a^2 t_\perp)^{-1}$ (a and $t_\perp$ are the nearest-neighbor distance and transfer integral, respectively, in the xy plane, where $t_\perp > t_\parallel$). By (2), this yields

$$\frac{\partial \ln\xi}{\partial p} = \frac{\partial \ln(t_\perp/t_\parallel)}{\partial p} B^{-1}(\xi) = -r\kappa B^{-1}(\xi) \; . \tag{13}$$

The last equality in (13) results from the assumption $t_\perp \propto \exp(-\lambda a)$, $t_\parallel \propto \exp(-\lambda d)$. κ is the isothermal compressibility, and $r = \frac{1}{3}\ln(t_\perp/t_\parallel)$. For realistic ratios $t_\perp/t_\parallel$ $(1 < t_\perp/t_\parallel < 20)$ we have $0 < r < 1$ and $-\kappa < \partial \ln(\xi)/\partial p < 0$. As expected,[20] with increasing pressure the FS anisotropy decreases, and a p-induced topological transition from the open to the closed FS can be realized.

For the calculation of the p dependence of T_{SF} we assume that q_c is not changed under pressure.[4] By (11), (2), and with $\partial \ln(S-1)/\partial p = S\,\partial \ln[IN_0(\varepsilon_F)]/\partial p$ we obtain

$$\frac{\partial \ln T_{SF}}{\partial p} = \frac{\partial \ln t_\parallel}{\partial p} + \frac{\partial \ln\xi}{\partial p}\left[1+\xi\frac{\partial \ln b}{\partial \xi}\right] + S\left[\frac{\partial \ln(t_\perp/I)}{\partial p} - [1-g(\xi)]\frac{1-\xi}{2-\xi}\frac{\partial \ln\xi}{\partial p}\right] . \tag{14}$$

Because of (13), $B(\xi) > 1$, and $\partial \ln(b)/\partial\xi < 0$, the S-independent contribution to (14) is positive. The second term in the wavy brackets vanishes for the open FS and gives a positive contribution for the closed FS. Since $\partial \ln(t_\perp/I)/\partial p > 0$, we obtain $\partial \ln(T_{SF})/\partial p > 0$. We point out that the p dependence of the Stoner factor $S(p)$ yields a considerable Stoner enhancement of $\partial \ln(T_{SF})/\partial p$. Let us consider a narrow band, i.e., small values of $t_\parallel$ and $t_\perp$, so that the transfer integrals are very sensitive to the application of pressure. In this case the inequality $\kappa \ll \partial \ln(T_{SF})/\partial p$, $\partial \ln\varepsilon_F/\partial p$ may hold. Then, the p dependence of T_{SF} essentially results from that of $t_\parallel$, $t_\perp/I$ and S; and the FS geometry has only a minor influence.

From (11) we get the p dependence of δ,

$$\partial \ln(\delta)/\partial p = \partial \ln(y)/\partial p - 3\,\partial \ln(T_{SF})/\partial p \; .$$

According to (13), $\partial \ln(y)/\partial p$ is determined by κ. Therefore, for a narrow band we get $\partial \ln(\delta)/\partial p < 0$, i.e., a suppression of SF effects under hydrostatic pressure.

We now relate the p dependence of T_{SF} and δ to that of γ, χ (zero-temperature magnetic susceptibility), and of the Wilson ratio $R = (\chi/\chi_0)(\gamma/\gamma_0)^{-1} = S(1+\lambda_{SF})^{-1}$. Thereby, we consider a narrow band and neglect the p dependence of ξ and y compared with that of ε_F, S, T_{SF}, and δ. Since $\gamma \simeq \gamma_0\lambda_{SF}(S)$ (for large enough S), $\gamma_0 \propto \varepsilon_F^{-1}$, and $T_{SF} \propto \varepsilon_F S^{-1}$, we obtain $\gamma \propto (1/S)\lambda_{SF}(S)T_{SF}^{-1}$. From (11) we have $\delta \propto T_{SF}^{-3}$, and for $\chi = \chi_0 S$, with $\chi_0 \propto \varepsilon_F^{-1}$, we get $\chi \propto T_{SF}^{-1}$. For $0 < \xi < 1$ and large S we have $\lambda_{SF} \propto \ln S$, so that χ does not scale with γ and R becomes large and p dependent, as in standard paramagnon theory. On the other hand, in Sec. III B we have found ξ and S parameter ranges, in particular within the coexistence region of AFM and FM SF's, for which the linear relationship $\lambda_{SF} \propto S$ holds. Under this condition the SF temperature T_{SF} is the only p-dependent energy scale for γ, δ, and χ. Expressing this p-dependent scaling in terms of γ, we obtain

$$\chi \propto \gamma, \quad \delta \propto \gamma^3; \quad T_{SF} \propto \gamma^{-1} \; . \tag{15}$$

Accordingly, the Wilson ratio is not large and does not depend on pressure.

V. DISCUSSION

The aim of this section is to discuss some approximations connected with our SF theory and to compare the results with several experimental data on UPt_3.

A. The use of the RPA

Here, we give a justification for the RPA description of low-temperature SF effects on C_v by considering the modifications resulting from the self-consistent renormalization (SCR) theory by Moriya and Kawabata (MK),[21] which takes into account the SF-SF coupling. In analogy with (3), we introduce the MK enhancement function $S^{MK}(\mathbf{q}) = \tilde{S}(\mathbf{q})(1+\lambda)^{-1}$; $\tilde{S}(\mathbf{q})$ is given by (3) with I replaced by $\tilde{I} = I(1+\lambda)^{-1}$, and λ resulting from a self-consistent calculation increases with I and T, where the temperature dependence dominates that of χ_0. In SCR, the condition (4) reads as $S^{MK} < S_m^{MK} = S_m(1+\lambda)^{-1}$. Taking small enough values of I we have $\lambda < 1$, and S_m^{MK} remains large enough. Concerning the SF contributions to C_v, in SCR we may start from (5) with λ added to the argument of the logarithm. Taking into account the considerable temperature dependence of λ, the leading C_v contribution at low T is given by (7) with $S(\mathbf{q})$ replaced by $S^{MK}(\mathbf{q})$, as shown by Makoshi and Moriya[22] for an isotropic band model. In SCR with a parabolic band, we obtain Eqs. (B1)–(B3) with S substituted by $\tilde{S}$ [except for the second term of (B2), in which $(S-1)/S = IN_0(\varepsilon_F)$ is used], which have essentially the same form as those of Ref. 22. There it was found that SCR (compared with RPA) yields a reduction of ΔC_v which becomes relevant above a characteristic temperature, increasing with decreasing S^{MK}. Summarizing, for small enough interaction parameters and temperatures, RPA provides a qualitatively correct description of the FS geometry effects on the SF contributions to C_v of exchange-enhanced paramagnetic metals.

B. Finite-wave-number spin-fluctuation effects

Let us discuss the influence of the finite-wave-number properties of SF's on the parameters γ, δ, and T_{SF} in (11) and on the range of validity of the $T^3 \ln T$ law.

Considering the mass enhancement, the behavior of

$\lambda_{SF}(S)$ in the region $1<\xi<2$ (Fig. 4), in particular the linear increase with S for $\xi \simeq 1.1$ and the concave S dependence for larger ξ values, is mainly caused by the peculiar $\mathbf{q}$ dependence of $\bar{\chi}_0(\mathbf{q})$ and $S(\mathbf{q})$, incorporating the combined effects of AFM and FM SF's. Note that for $0<\xi<1$ convex functions $\lambda_{SF}(S)$ are obtained. More results and discussions are given in Ref. 23. Our analysis shows that the mass enhancement depends very sensitively on the finite-wave-number properties of $\bar{\chi}_0(\mathbf{q})$, as was also stressed by Coffey and Pethick.[5] Ignoring, for example, the $\mathbf{q}$ dependence of $\bar{\chi}_0(\mathbf{q})$ for the closed FS [approximation $S(\mathbf{q})=S$ in (9)], the behavior of λ_{SF} is qualitatively changed into the linear relationship $\lambda_{SF}\propto S$ (for $S\gg 1$). Therefore, in general this approximation (employed, e.g., in Ref. 24) is not justified.

As to the sensitivity of the SF contributions (8) beyond γT to finite-wave-number effects, firstly we have found[23] that the magnitude of the $T^3 \ln T$ coefficient δ is not affected by the structure of $S(\mathbf{q})$ and by the choice of q_c. This is in accord with the parabolic-band result in the framework of Fermi-liquid[5] and paramagnon models (Appendix B). Therefore, the approximation $S(\mathbf{q})=S$ (Ref. 19) employed in Sec. III C gives the correct δ value. The calculation of T_{SF} from (10) using the full $\mathbf{q}$ dependence of $S(\mathbf{q})$ (Ref. 23) shows a decrease of T_{SF} compared with (11). Taking $q_c=1.6$ and, for example, $\xi=1.1$, the value of $b=T_{SF}/\bar{T}_F$ decreases by about 40% and 50% for $S=4$ and $S=6$, respectively. Such a rather sensitive dependence of T_{SF} on the finite-wave-number properties of SF's was also found in the Fermi-liquid SF model by Coffey and Pethick.[5]

Finally, we comment on the temperature range of validity of the $T^3 \ln T$ law. At very low temperatures, $T \ll T_m$, the $T^3 \ln T$ term is the leading-order contribution in a low-temperature expansion and results from long-wavelength SF's with $|\mathbf{q}|\simeq 0$ (including the anisotropic FM SF's described in Sec. II). The contribution of those SF's to C_v may be obtained from (10) taking a cutoff energy $\varepsilon_0 \ll \varepsilon_c$ (note that ε_c with $q_c=1.6$ is rather high). At elevated temperatures shorter-wavelength SF's are excited; their contribution to C_v can be evaluated from (10) by integrating over wave numbers belonging to energies from ε_0 to ε_c. We have found that this contribution reveals a $T^3 \ln T$ law in an intermediate temperature range. Recently, a similar behavior was obtained in the localized-paramagnon model by Konno and Moriya.[25] Note that our result is consistent with the fact that AFM SF's do not give rise to a $T^3 \ln T$ term at very low temperatures, but only to higher-order contributions in a low-temperature expansion.[16] A more detailed analysis of this problem will be given in a forthcoming paper. The sum of the long-wavelength and shorter-wavelength SF contributions just discussed yields the $T^3 \ln T$ law for $0<T<T_m$ obtained in Sec. III C. The inclusion of the $\mathbf{q}$ dependence of $S(\mathbf{q})$ results in a decrease of $T_m/\bar{T}_F$ compared with (11) by about the same percentage as $T_{SF}/\bar{T}_F$.[23]

C. Anisotropic spin-fluctuation model for UPt_3

In this section we suggest an anisotropic SF model for UPt_3 by comparing the results of our SF theory with several relevant experimental data.

Concerning the structure of narrow quasiparticle bands in UPt_3 near ε_F, de Haas–van Alphen measurements[26] have directly shown that heavy-quasiparticle bands exist and that the FS relevant for our model [strongly anisotropic $\Gamma 3$ FS with the largest cyclotron mass ($90m_e$) and of dominantly $5f$ character] is closed. The quasiparticle band structure derived by Marabelli and Wachter[27] from far-infrared and point contact spectroscopies consists of two very narrow (4–5 meV) quasiparticle bands of predominantly $5f$ character which are hybridized with a wide d band and separated by a pseudogap of about 4 meV, where ε_F lies in the upper subband. Compared with this model our single-band model refers to the upper subband which is the essential one in the study of SF phenomena at low temperatures (smaller than the pseudogap energy, i.e., $T<50$ K). To perform a comparison between theory and experiments, we adapt our single-band model (for a lattice without basis) to the crystal structure of UPt_3 (hcp lattice with $c/a=0.85$ and $a=5.76$ Å, and a basis of two U ions belonging to adjacent basal planes) by the following simplification: We consider the underlying structure to be effectively simple hexagonal with a primitive cell reduced along the c axis by a factor of two; i.e. we take $d=c/2$. In Appendix C we extend the band model by describing a finite bandwidth.

Recently, magnetic neutron scattering measurements on UPt_3 at low temperatures have revealed AFM SF's around $\mathbf{Q}=(0,0,2\pi/c)$, corresponding to AFM correlations between U spins in adjacent basal planes,[11,12] as well as FM SF's within the same basal plane.[12] Those experiments may be explained by our anisotropic SF model in the closed-FS region $1<\xi<2$ which describes the coexistence of exchange-enhanced AFM SF's around $\mathbf{Q}=(0,0,\pi/d)$ ($d=c/2$, see above) and of FM SF's perpendicular to the hexagonal axis (cf. Sec. II). The neutron-scattering cross section (for $k_B T \ll \omega$) is proportional to $\mathrm{Im}\chi(\mathbf{q},\omega)$ which, in the paramagnon approach, is given by

$$\mathrm{Im}\chi(\mathbf{q},\omega)=\frac{1}{I}S(\mathbf{q})\Gamma(\mathbf{q})\frac{\omega}{\omega^2+\Gamma^2(\mathbf{q})} \quad \text{for } \omega \ll \frac{\hbar^2}{m_b d}|\mathbf{q}| , \tag{16}$$

where

$$\Gamma(\mathbf{q})=\bar{T}_F\left[\frac{4\pi^2}{d_\parallel}\xi\frac{S(\mathbf{q})}{S}\bar{u}(\mathbf{q})\right]^{-1}$$

is the SF energy. Concerning the ω dependence, (16) shows a maximum at $\omega_m=\Gamma(\mathbf{q})$ and adequately describes the constant-$\mathbf{q}$ spectra ("single-pole" approximation[11,12]).

As to the $\mathbf{q}$ dependence, there are some complications connected with the non-Bravais lattice of UPt_3. Firstly, the neutron spectra at reciprocal-lattice vectors (e.g., $\mathbf{Q}$, $2\mathbf{Q}$) probe the static susceptibility and the SF energy, which are periodic in the extended-zone representation, at the Brillouin-zone center, whereas in our simplified (Bravais lattice based) model the maximum in the susceptibility occurs at the zone boundary. Moreover, the $\mathbf{q}$ dependence of the cross section is mainly determined by the magnetic structure factor (originating from the two U ions per primitive unit cell) and by the U $5f$ form factor.[28] Therefore, it is hardly justified to extract quantitative information on the q_z dependence of the static susceptibility in single-band models from the existing neutron data, as was done in Refs. 24 and 29. A further problem is raised by the behavior of $\Gamma(\mathbf{q})$, which is found to be nearly independent of $\mathbf{q}$,[11,12] which cannot be explained by paramagnon theory. Note that (16) is only valid for $|\mathbf{q}| \gg \omega m_b d/\hbar^2$, and for $\mathbf{q}=0$, $\omega \neq 0$ we have $\mathrm{Im}\chi(0,\omega)=0$. In spite of this deficiency, we assume that the neutron spectra at large enough wave numbers may be described by the paramagnon approach, and we take the experimental value[11] $\Gamma(\mathbf{Q})=5$ meV for a further comparison of the theory with experiments.

Experimentally, for C_v the law (11) was found in a wide range of temperatures (extending up to about 20 K),[1,7] where $\gamma=422$ mJ/mol K^2 and $\delta=1.38$ mJ/mol K^4.[7] Using the experimental values of Γ, γ, and δ, let us estimate our SF model parameters and other relevant quantities. With $q_c=1.6, \Gamma(\mathbf{Q})$ from (16) $[\bar{u}(\mathbf{Q})=1/4\pi^2]$, and δ rewritten as $\delta=(36/\pi)(S-1)\gamma A(\xi)/(1+\lambda_{\mathrm{SF}})\bar{T}_F^2$, we obtain the parameters S, ε_F, and γ_0 as functions of ξ. From those values the Wilson ratio and the SF temperature are calculated; for $1.1 \le \xi \le 1.9$ we find $1.45 \ge R \ge 1.26$ and $17 \ge T_{\mathrm{SF}} \ge 14$ K. A rather good agreement with experiments [$R=1.47$ (Ref. 30), $T_{\mathrm{SF}}=27$ K (Ref. 7)] is found for the choice $\xi=1.1$ which we use hereafter. We get $S=3.7$, $\varepsilon_F=0.77$ meV, $\gamma_0=166.8$ mJ/mol K^2; $R=1.45, T_{\mathrm{SF}}=17$ K. The moderate value of S corresponds to the enhancement factor $S(\mathbf{Q})=7.1$ for the AFM SF's along the hexagonal axis. The rather large γ_0 value expresses the fact that our model starts from a narrow heavy-quasiparticle band. The very good agreement of R with the experimental value should be contrasted with the following puzzle encountered in the Fermi-liquid analysis (in the parabolic model).[5-7] To fit γ and δ [with $k_F=1.06$ Å^{-1} (Ref. 7)] requires a large negative amplitude A_0^a ($A_0^a=-3.7$) which yields a much too high Wilson ratio ($R=4.7$); or equivalently, the magnetic susceptibility ($R \simeq 1.5$) suggests that $A_0^a \simeq -\frac{1}{2}$, which results in a magnitude of δ more than 100 times smaller than the observed coefficient. Concerning T_{SF}, we remark that the difference between the theoretical and experimental values may be reduced by a fit procedure including q_c (T_{SF} increases with q_c); besides, there is a large scatter in the observed T_{SF} values. From our estimate, the temperature range of validity of the $T^3 \ln T$ law is given by $T_m \simeq 3$ K, indicating that further investigations are required to get a better agreement between theory and experiment. Checking the consistency of the parameter estimate with the condition (16) for ω and $|\mathbf{q}|$ near 5 meV and $|\mathbf{Q}|=\pi/d$, respectively, we get $\hbar^2/m_b d^2=11.5$ meV; that is, the use of (16) to compare $\Gamma(\mathbf{Q})$ with the neutron-scattering result is justified within our approach.

Considering the dimensions of the anisotropic FS let us emphasize that we obtain $d_\parallel/d_\perp=1.38$, which agrees well with the mean ratio of 1.25 obtained, for the $\Gamma 3$ FS, by band structure calculations.[17]

High-pressure experiments[4,7] yield the strong p dependencies $\partial \ln(T_{\mathrm{SF}})/\partial p \simeq 30$ Mbar^{-1}, $\partial \ln(\delta)/\partial p \simeq -10^2$ Mbar^{-1} (only the order of magnitude can be well established), and $\partial \ln\gamma/\partial p \simeq \partial \ln\chi/\partial p \simeq -27$ Mbar^{-1}. We have[7] $\kappa=0.48$ Mbar$^{-1} \ll \partial \ln T_{\mathrm{SF}}/\partial p$ which corresponds to the narrow-band case discussed in Sec. IV (neglect of the p dependence of ξ and y). The essential observation is that the given p derivatives are in accord with the scaling relations (15), provided that $\lambda_{\mathrm{SF}} \propto S$. Such a linear relationship was just found for $\xi=1.1$ and $S<S_m$ (Fig. 4). That means our SF model may explain the high-pressure experiments. It should be stressed that the scaling (15) was previously considered to be the strongest evidence against the standard paramagnon picture of UPt_3.[8,31] Within our extended SF theory, this scaling merely rules out the FS region $0<\xi<1$ ($\lambda_{\mathrm{SF}} \propto \ln S$ for large S).

Very recently,[14] neutron-scattering experiments at very low energy transfers ($\simeq 0.5$ meV) have revealed long-range AFM order below $T_N=5$ K connected with a doubling of the unit cell in the basal planes. This finding seems not to be related to the AFM SF's along the hexagonal axis probed at higher energy transfers ($\simeq 5$ meV).[11,12] In view of this new result, the applicability of our SF theory to UPt_3 is restricted to $T>T_N$, where higher-energy (shorter-wavelength) SF's, in particular the AFM SF's described by the theory, may be excited and play a dominant role.

VI. CONCLUSIONS

The essential features and results of the present analysis of FS geometry effects on the SF behavior of exchange-enhanced paramagnetic metals are the following.

(i) The basic model in our RPA paramagnon approach is the anisotropic band dispersion (1) which yields anisotropic FS of different topology, the $\chi_0(\mathbf{q})$ model showing various analytical structures, and qualitatively novel SF phenomena compared with isotropic paramagnon models.

(ii) Among different kinds of exchange-enhanced SF's, our model describes the coexistence of anisotropic AFM and FM SF's.

(iii) The $T^3 \ln T$ law for C_v is affected by FS geometry in two ways: The amplitude is enlarged compared with the parabolic band model, and the temperature range of validity increases with FS anisotropy.

(iv) The structure of $\chi_0(\mathbf{q})$ can lead to a linear relation between the SF-mediated mass enhancement and the Stoner factor which results in the pressure dependent scaling (15).

(v) The comparison between theory and experiments on UPt_3 (combining neutron data with thermodynamic properties) yields a good agreement. From this an anisotropic SF model for UPt_3 is proposed, and we conclude that our model incorporates essential aspects of anisotropic fluctuation phenomena.

Let us point out that our anisotropic model for the static susceptibility results from the dispersion (1) and the corresponding FS model and is not introduced independently, as in some recent studies of SF-mediated superconductivity.[24,29,32] The anisotropic nature of SF plays a decisive role in determining the SF-mediated superconducting pairing interaction in heavy-fermion superconductors.[29,32–34] Beál-Monod *et al.*[33] have qualitatively discussed the possible "mixture of nearly FM and AFM tendencies" which is similar to the coexistence of FM and AFM SF's described by our model.

Finally, it should be stressed that, in the application to heavy-fermion metals, our simplified theory has only model character, but demonstrates the important role of anisotropy effects on low-energy fluctuations. In a more realistic model one has to take into account band-structure effects not only by an anisotropic and nonparabolic band dispersion, but also by at least two bands. Very recently, Auerbach *et al.*,[8,13] within their Kondo boson theory (based on an extended f^0-f^1 Anderson lattice model including spin-orbit and crystal-field effects and yielding the same scaling behavior as our theory), have found that $\mathrm{Im}\chi(\mathbf{q},\omega)$ shows an AFM peak and does not vanish at $\mathbf{q}=\mathbf{0}$ (for $\omega\neq 0$) as observed in neutron scattering. This behavior is caused by spin-flip scattering and cannot be obtained from the single-band Hubbard model. In light of our investigations, the Kondo boson approach should be improved by including the uniaxial anisotropy relevant in hexagonal UPt_3. This also refers to the recent theory of the f^1-f^2 Anderson lattice by Brandow,[35] which yields a peak of $\mathrm{Im}\chi(\mathbf{q},\omega)$ at the zone boundary attributed to the hybridized band structure.

ACKNOWLEDGMENT

We would like to thank B. Lippold, I. Mertig, P. Wachter, and W. Weller for valuable discussions.

APPENDIX A: RESPONSE FUNCTION $\chi_0(\mathbf{q},\omega)$

We consider the response function of noninteracting electrons at zero temperature,

$$\chi_0(\mathbf{q},\omega)=\sum_{\mathbf{k}}\frac{\Theta(\varepsilon_F-\varepsilon_{\mathbf{k}+\mathbf{q}})-\Theta(\varepsilon_F-\varepsilon_{\mathbf{k}})}{\omega-\varepsilon_{\mathbf{k}+\mathbf{q}}+\varepsilon_{\mathbf{k}}+i\varepsilon}\ , \tag{A1}$$

with $\varepsilon_{\mathbf{k}}$ given by (1). From (A1) we calculate the anisotropic static susceptibility $\bar{\chi}_0(\mathbf{q})=\chi_0(\mathbf{q})/\chi_0(0)$. With the notation given in Sec. II, $\bar{\chi}_0(\mathbf{q})$ can be expressed by the one-dimensional integral

$$\bar{\chi}_0(q_\perp,q_\parallel)=1+\frac{4}{d_\parallel q_\perp^2}\left[\sin\left[\frac{d_\parallel}{2}\right](1-\cos q_\parallel)-\int_{-d_\parallel/2}^{d_\parallel/2}dk_z\,\mathrm{sgn}(a)\Theta(a^2-b^2)(a^2-b^2)^{1/2}\right]\ , \tag{A2}$$

where

$$a=\tfrac{1}{2}[\tfrac{1}{2}q_\perp^2+\cos k_z-\cos(k_z+q_\parallel)],\quad b^2=\tfrac{1}{2}q_\perp^2(\xi-1+\cos k_z)\ .$$

In I we have derived closed-form expressions for $\bar{\chi}_0(q_\perp,q_\parallel)$ with $q_\perp=0$ or $q_\parallel=0$. Since the closed-FS region $\xi<2$ plays a central role in this paper, we quote the result for $\bar{\chi}_0(0,q_\parallel)$ (correcting two misprints in I),

$$\bar{\chi}_0(0,q_\parallel)=1+[d_\parallel\sin(\tfrac{1}{2}q_\parallel)]^{-1}\left[\cos(\tfrac{1}{2}d_\parallel)\ln\left|\frac{\sin(\frac{1}{2}d_\parallel)-\sin(\frac{1}{2}q_\parallel)}{\sin(\frac{1}{2}d_\parallel)+\sin(\frac{1}{2}q_\parallel)}\right|+\cos(\tfrac{1}{2}q_\parallel)\ln\left|\frac{\sin(\frac{1}{2}q_\parallel+\frac{1}{2}d_\parallel)}{\sin(\frac{1}{2}q_\parallel-\frac{1}{2}d_\parallel)}\right|\right]\ . \tag{A3}$$

By (A2) the numerical calculation of the full $\mathbf{q}$ dependence of $\bar{\chi}_0(\mathbf{q})$ yields the following results. $\bar{\chi}_0(\mathbf{q})$ reveals a maximum at $\mathbf{q}=\mathbf{0}$ for $0<\xi<1$ or at $\mathbf{Q}=(0,0,\pi)$ for $1<\xi<2$ [Fig. 2(a)]. For the open FS ($\xi>2$), $\bar{\chi}_0(\mathbf{q})$ is constant in the finite volume Ω_c of the $\mathbf{q}$ space (see II).

The spectral density governing the low-frequency SF's is given by $\mathrm{Im}\chi_0(\mathbf{q},\omega)\simeq\omega u(\mathbf{q})$ for $\omega/|\mathbf{q}|\ll 1$, where in I analytical results for $u(\mathbf{q})$ with $|\mathbf{q}|\ll 1$ are derived for all ξ. Introducing $\bar{u}(\mathbf{q})=(d^3/\Omega)\alpha u(\mathbf{q})$, for $\xi<2$ we get

$$\bar{u}(\mathbf{q})=\{\pi^2 q_\parallel[2(z_1-z_2)]^{1/2}\}^{-1}K\left[\frac{(z_1-1)(z_2+1)}{2(z_1-z_2)}\right]^{1/2}\ ,$$
$$z_{1,2}=-\left[\frac{q_\perp}{q_\parallel}\right]^2\pm\left[1-2(\xi-1)\left[\frac{q_\perp}{q_\parallel}\right]^2+\left[\frac{q_\perp}{q_\parallel}\right]^4\right]^{1/2}\ . \tag{A4}$$

$K(k)$ is the complete elliptic integral of the first kind. Besides the $|\mathbf{q}|^{-1}$ divergence of $\bar{u}(\mathbf{q})$ for $|\mathbf{q}|\to 0$, there are additional pronounced structures. For $\xi<2$, $|\mathbf{q}|\bar{u}(\mathbf{q})$ shows a maximum at $q_\perp\simeq q_\parallel$. For $\xi>2$ a logarithmic divergence of $|\mathbf{q}|\bar{u}(\mathbf{q})$ at $\mathbf{q}$ directions parallel to the tangent in the parabolic points on the FS (*X*-type Taylor anomaly) occurs.[36] For finite wavevectors, logarithmic divergences of $\bar{u}(\mathbf{q})$ on the Taylor anomaly surface appear.[37]

APPENDIX B: PARAMAGNON CONTRIBUTIONS TO THE SPECIFIC HEAT IN THE PARABOLIC BAND MODEL

For the evaluation of the C_v contributions (7) due to FM SF's with $|\mathbf{q}|\ll 1$ in the parabolic band model $\varepsilon_k=k^2/2m_b$, we use the expansions $u(\mathbf{q})=N_0(\varepsilon_F)\pi k_F(4\varepsilon_F q)^{-1}$ with $N_0(\varepsilon_F)=\Omega m_b k_F/2\pi^2\hbar^2$ and, in the expression for λ_{SF}, $\chi_0(\mathbf{q})=N_0(\varepsilon_F)(1-q^2/12k_F^2)$, whereas in the second term of (7) we take the approximation $S(\mathbf{q})=S$.[19] Then, for the paramagnon contributions to C_v we obtain the low-temperature expansion

$$\frac{\Delta C_v}{C_{v0}}=\lambda_{\rm SF}+\tfrac{3}{5}\pi^2(S-1)\left[\frac{T}{\overline{T}_F}\right]^2\ln\left[\frac{T}{\overline{T}_{\rm SF}}\right], \quad \text{(B1)}$$

$$\lambda_{\rm SF}=\tfrac{9}{2}\ln[1+\tfrac{1}{12}(S-1)q_c^2]-\tfrac{3}{8}\frac{(S-1)}{S}q_c^2, \quad \text{(B2)}$$

$$\overline{T}_F=\frac{4\varepsilon_F}{\pi(S-1)},\quad T_{\rm SF}=e^{-\eta}q_c\overline{T}_F,\quad \eta=1.44\,. \quad \text{(B3)}$$

q_c is a cutoff wave number in units of k_F. Note that our result differs from that obtained by Brinkman and Engelsberg:[19] The coefficient of the logarithmic term given by those authors (in their language only the "fermion contribution" is taken into account) is larger than our value by a factor of $3(S-1)/S$, the second term in (B2) is neglected in Ref. 19 (limit of large S), and $\eta_{\rm BE}=1.78$. Our value for η agrees with that found by Coffey and Pethick.[5]

APPENDIX C: FINITE-BANDWIDTH EFFECTS

Here, we outline the extension of the SF model for UPt_3 concerned with the description of a finite bandwidth. We approximate the Brillouin zone for the simple hexagonal lattice ($d=c/2$) of volume $\Omega_{\rm BZ}=16\pi^3(\sqrt{3}a^2d)^{-1}$ by a circular cylinder of equal volume, i.e., of height $2\pi/d$ and radius $k_c=2(2\pi/\sqrt{3})^{1/2}a^{-1}=1.62d^{-1}$. Similar to the approach by MacDonald[38] for the parabolic band model, we introduce a cutoff in the basal-plane dispersion which we take as k_c,

$$\varepsilon_{\bf k}=\frac{\hbar^2}{2m_b}(k_x^2+k_y^2)\Theta(k_c-k_\perp)-2t_\parallel\cos(k_zd)\,, \quad \text{(C1)}$$

where $k_\perp=(k_x^2+k_y^2)^{1/2}$. For the density of states $N_0(\varpi)$, $\varpi=\omega/2t_\parallel$, we obtain

$$\frac{4\pi^2\hbar^2 d}{\Omega m_b}N_0(\varpi)=\begin{cases} d_\parallel(\varpi), & -1<\varpi<\Delta-1\\ d_\parallel(\varpi)-2\cos^{-1}(\Delta-\varpi), & \Delta-1<\varpi<\Delta+1\,,\end{cases} \quad \text{(C2)}$$

where $\Delta=(k_cd)^2/2\alpha=1.31/\alpha$ and

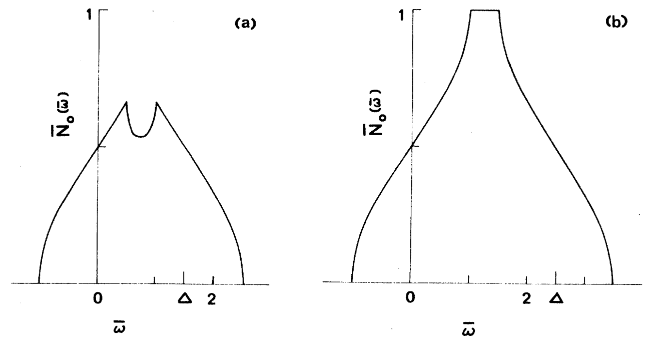

FIG. 7. Density of states (C2), where $\overline{N}_0(\varpi)=2\pi\hbar^2d(\Omega m_b)^{-1}N_0(\varpi)$, for (a) $\Delta=1.5$, (b) $\Delta=2.5$.

$$d_\parallel(\varpi)=2\cos^{-1}(-\varpi)\Theta(1-\varpi)+2\pi\Theta(\varpi-1)\,.$$

In Fig. 7, $N_0(\varpi)$ is shown for two characteristic Δ values [for $\Delta>2$ a plateau in $N_0(\varpi)$ appears]. Note that $N_0(\varpi)$ is symmetric with respect to $\varpi=\frac{1}{2}\Delta$, and the cutoff k_c results in the bandwidth $W=2t_\parallel(\Delta+2)$.

Using the model parameters estimated in Sec. V C we obtain $2t_\parallel=7.7$ meV, $\alpha=0.67$, $\Delta=1.95$, and $W=30.5$ meV. Relating the value of W to the bandwidth in the model of Ref. 27 ($\simeq 5$ meV) describing the fully dressed heavy quasiparticles, we point out that, in our model for the heavy quasiparticles, $N_0(\varpi)$ does not contain the SF-induced renormalization so that $W>5$ meV. For a detailed comparison the calculation of the SF-renormalized density of states is required. Such a calculation, however, was not performed. Comparing W with the intrasite quasiparticle interaction U, we get $U=20.7$ meV and $U/W=0.68$, which nearly agrees with $IN_0(\varepsilon_F)=0.73$, as expected from a rough estimate.

The finite-bandwidth dispersion (C1) leads to a reduction of the static susceptibility [compared with (A2), Fig. 2(a)] which appears for $|{\bf q}|>|{\bf q}_0|$ (for $q_\parallel=0$ we get $|{\bf q}_0|/\sqrt{8}\xi=k_cd/\sqrt{8\alpha}\xi-0.5=0.17$) and increases with $|{\bf q}|$; however, a detailed calculation of $\overline{\chi}_0({\bf q})$ for the model (C1) was not performed. Note that the function $\overline{u}({\bf q})$ for $|{\bf q}|\ll 1$ [Eq. (A4)] is not affected by the cutoff. Within our calculations based on the model (1), the band cutoff is effectively taken into account by the parameter q_c.

[1]For an experimental review, see G. R. Stewart, Rev. Mod. Phys. **56**, 755 (1984).
[2]For theoretical reviews, see P. A. Lee, T. M. Rice, J. W. Serene, L. J. Sham, and J. W. Wilkins, Commun. Condensed Matter Phys. **12**, 99 (1986); P. Fulde, J. Keller, and G. Zwicknagl, Solid State Phys. **47**, 1 (1988).
[3]D. Fay and J. Appel, Phys. Rev. B **32**, 6071 (1985).
[4]G. E. Brodale, R. A. Fisher, N. E. Phillips, G. R. Stewart, and A. L. Giorgi, Phys. Rev. Lett. **57**, 234 (1986).
[5]D. Coffey and C. J. Pethick, Phys. Rev. B **33**, 7508 (1986).
[6]C. J. Pethick and D. Pines, in Proceedings of the IVth International Conference on Recent Progress in Many-Body Theories, edited by P. Siemens and R. Smith (Springer, Berlin, in press); C. J. Pethick, D. Pines, K. F. Quader, K. S. Bedell, and G. E. Brown, Phys. Rev. Lett. **57**, 1955 (1986).
[7]A. de Visser, A. Menovsky, and J. J. M. Franse, J. Magn. Magn. Mater. **63&64**, 365 (1987); Physica B+C **147B**, 81 (1987), and references therein.
[8]A. Auerbach and K. Levin, Phys. Rev. Lett. **57**, 877 (1986); Phys. Rev. B **34**, 3524 (1986); J. Appl. Phys. **61**, 3162 (1987).
[9]J. W. Rasul and A. P. Harrington, J. Phys. C **20**, 4783 (1987); J. W. Rasul and H. U. Desgranges, J. Phys. C **19**, L671 (1986).
[10]A. J. Millis, Phys. Rev. B **36**, 5420 (1987).
[11]G. Aeppli, A. Goldman, G. Shirane, E. Bucher, and M.-Ch.

Lux-Steiner, Phys. Rev. Lett. **58**, 808 (1987).
[12]A. I. Goldman, G. Shirane, G. Aeppli, E. Bucher, and J. Hufnagl, Phys. Rev. B **36**, 8523 (1987).
[13]A. Auerbach, J. H. Kim, K. Levin, and M. R. Norman, Phys. Rev. Lett. **60**, 623 (1988); A. Auerbach, J. H. Kim, and K. Levin, Physica B+C **148B**, 50 (1987).
[14]G. Aeppli, E. Bucher, C. Broholm, J. K. Kjems, J. Baumann, and J. Hufnagl, Phys. Rev. Lett. **60**, 615 (1988).
[15]For a review, see P. C. E. Stamp, J. Phys. F **15**, 1829 (1985).
[16]T. Moriya, Phys. Rev. Lett. **24**, 1433 (1970); T. Moriya and T. Kato, J. Phys. Soc. Jpn. **31**, 1016 (1971).
[17]T. Oguchi and A. J. Freeman, J. Magn. Magn. Mater. **52**, 174 (1985); **61**, 233 (1986); C. S. Wang, M. R. Norman, R. C. Albers, A. M. Boring, W. E. Pickett, H. Krakauer, and N. E. Christensen, Phys. Rev. B **35**, 7260 (1987).
[18]H. Fehske and D. Ihle, J. Phys. F **17**, 2109 (1987); J. Phys. F **18**, 33 (1988).
[19]W. F. Brinkman and S. Engelsberg, Phys. Rev. **169**, 417 (1968).
[20]I. M. Lifshitz, Zh. Eksp. Teor. Fiz. **38**, 1569 (1960).
[21]T. Moriya and A. Kawabata, J. Phys. Soc. Jpn. **34**, 639 (1973); **35**, 669 (1973).
[22]K. Makoshi and T. Moriya, J. Phys. Soc. Jpn. **38**, 10 (1975).
[23]H. Fehske and D. Ihle, J. Phys. C **21**, 4663 (1988).
[24]M. R. Norman, Phys. Rev. Lett. **59**, 232 (1987).
[25]R. Konno and T. Moriya, J. Phys. Soc. Jpn. **56**, 3270 (1987).
[26]L. Taillefer, R. Newbury, G. G. Lonzarich, Z. Fisk, and J. L. Smith, J. Magn. Magn. Mater. **63&64**, 372 (1987); L. Taillefer and G. G. Lonzarich, Phys. Rev. Lett. **60**, 1570 (1988).
[27]F. Marabelli, P. Wachter, and J. J. M. Franse, J. Magn. Magn. Mater. **62**, 287 (1986); F. Marabelli and P. Wachter, *ibid.* **70**, 364 (1987).
[28]W. Marshall and S. W. Lovesey, *Theory of Thermal Neutron Scattering* (Clarendon, Oxford, 1971).
[29]W. Putikka and R. Joynt, Phys. Rev. B **37**, 2372 (1988).
[30]P. H. Frings and J. J. M. Franse, Phys. Rev. B **31**, 4355 (1985).
[31]O. T. Valls and Z. Tešanović, Phys. Rev. Lett. **53**, 1497 (1984).
[32]K. Miyake, S. Schmitt-Rink, and C. M. Varma, Phys. Rev. B **34**, 6554 (1986); C. M. Varma, Physica B+C **148B**, 17 (1987).
[33]M. T. Béal-Monod, C. Bourbonnais, and V. J. Emery, Phys. Rev. B **34**, 7716 (1986).
[34]D. J. Scalapino, E. Loh, Jr., and J. E. Hirsch, Phys. Rev. B **34**, 8190 (1986); **35**, 6694 (1987).
[35]B. H. Brandow, Phys. Rev. B **37**, 250 (1988).
[36]In Ref. 18 (I), Eq. (23) for $\gamma_{c1} < \gamma < \gamma_{c2}$, the unity in the argument of the elliptic integral has to be replaced by α^2.
[37]M. I. Kaganov, A. G. Plyavenek, and M. Hietschold, Zh. Eksp. Teor. Fiz. **82**, 2030 (1982).
[38]A. H. MacDonald, Phys. Rev. B **24**, 1130 (1981).